ÓPTICA PURA Y APLICADA
www.sedoptica.es

Type: Research paper
Section: Sensors and Photonic Devices

Coherent perfect absorption in epsilon-near-zero ITO thin film in near infrared

Perfecta absorción coherente en película delgada de ITO con épsilon casi cero en el infrarrojo cercano

Md. Alamgir Badsha[1*], Mohammad Abdur Rashid[1], Md. Humaun Kabir[1], Md. Mehade Hasan[1]

1. Department of Physics, Jashore University of Science and Technology, Jashore-7408, Bangladesh.
(*) E-mail: alamgir93_phy@just.edu.bd
S: miembro de SEDOPTICA / SEDOPTICA member

Received: 29/08/2019 Accepted: 14/03/2020
DOI: 10.7149/OPA.53.1.51031

ABSTRACT

Perfect absorption is one of the important application of epsilon-near-zero (ENZ) material. We analyze here the coherent perfect absorption (CPA) in single and bilayer of ENZ thin film of ITO by admittance matching method. To enhance the absorption, a coupling layer of dielectric is to deposit on the substrate with an ENZ ITO layer. CPA conditions are presented here in simulation results which are obtained for p-polarized light. This mode is comparable with the transverse resonance effect. In order to obtain the symmetric results, the optimum polarization direction of illumination is also extracted here. Employing the ENZ CPA property of ITO, this structure is applicable in optical switching, modulation and sensor at the telecommunication regime.

Keywords: Absorption, Epsilon-near-zero, Coupling layer, Modulation, Optical switching.

REFERENCES AND LINKS:

[1] Md. Alamgir Badsha, Young Chul Jun, Chang Kwon Hwangbo, "Admittance matching analysis of perfect absorption in unpatterned thin films," Optics Communications **332**, 206-213 (2014).
[2] Gururaj V. Naik , Vladimir M. Shalaev , Alexandra Boltasseva. "Alternative Plasmonic Materials: Beyond Gold and Silver," Adv. Mater. **25**, 3264–3294 (2013).
[3] A. Monti, F. Bilotti, A. Toscano, Lucio Vegni, "Possible implementation of epsilon-near-zero metamaterials working at optical frequencies," Optics Communications **285**, 3412-3418 (2012).
[4] N. Garcia, E. V. Ponizovskaya, John Q. Xia, "Zero permittivity materials: Band gaps at the visible," Applied Physics Letters **80**, 1120-1122 (2002).
[5] Richard W. Ziolkowski, "Propagation in and scattering from a matched metamaterial having a zero index of refraction," Physical Review E **70**, 046608 (2004).
[6] Aaron J. Pung , Michael D. Goldflam , D. Bruce Burckel , Igal Brener , Salvatore Campione, "Enhancing Absorption Bandwidth through Vertically Oriented Metamaterials," Applied Science **9** (11), 2223 (2019).
[7] M. Silveirinha, N. Engheta, "Tunneling of Electromagnetic Energy through Subwavelength Channels and Bends using ε-Near-Zero Materials," Physical Review Letters **97**, 157403 (2006).
[8] M. G. Silveirinha, N. Engheta, "Theory of Supercoupling Squeezing Wave Energy. Field Confinement in Narrow Channel and Tight Bends Using Epsilon-Near-Zero Metamaterials," Physical Review B **76**, 245109 (2007).
[9] B. Edwards, Andrea Alù, M. Young, M. Silveirinha, Nader Engheta, "Experimental Verification of ε-Near-Zero Metamaterial Supercoupling and Energy Squeezing Using a Microwave Waveguide," Physical Review Letters **100** (3), 033903 (2008).

 © Sociedad Española de Óptica

[10] R. Liu, Q. Cheng, T. Hand, J. J. Mock, T. J. Cui, S. A. Cummer, D. R. Smith, "Experimental emonstration of Electromagnetic Tunneling Through an Epsilon-Near-Zero Metamaterial at Microwave Frequencies," Physical Review Letters **100** (3), 023903 (2008).
[11] Q. Cheng, R. Liu, D. Huang and T. J. Cui, D. R. Smith, "Circuit verification of tunneling effect in zero permittivity medium," Applied Physiscs Letters **91**, 234105 (2007).
[12] Andrea Alu, M. G. Silveirinha, A. Salandrino and N. Enghet, "Epsilon-near-zero metamaterials and electromagnetic sources: Tailoring the radiation phase pattern," Physical Review B **75**, 155410 (2007).
[13] J. Bai, S. Shi, and D. W. Prather, "Analysis of epsilon-near-zero metamaterial super-tunneling using cascaded ultra-narrow waveguide channels," Progress In Electromagnetics Research M **14**, 113-121 (2010).
[14] R. J. Pollard, A. Murphy, W. R. Hendren, P. R. Evans, R, Atkinson, G. A. Wurtz, A. V. Zayats, "Optical Nonlocalities and Additional Waves in Epsilon-Near-Zero Metamaterials," Phyiscal Review Letters **102**, 127405 (2009).
[15] Andrea Alu, M. G. Silveirinha, N. Engheta, "Transmission-line analysis of ε-near-zero-filled narrow channels," Physical Review E **78**, 016604 (2008).
[16] Simin Feng, Klaus Halterman, "Coherent perfect absorption in epsilon-near-zero metamaterials," Physical Review B **86**, 165103 (2012).
[17] K. Halterman, J. Merie Elson, "Near-perfect absorption in epsilon-near-zero structures with hyperbolic dispersion" Optics Express **22(6)**, 7337-7348 (2014).
[18] Simin Feng, "Dual-Band Coherent Perfect Absorption/Thermal Emission From Ultrathin Bilayers," Advanced Electromagnetics **2(3)**, 22-27 (2013).
[19] Nadav Gutman, Andrey A. Sukhorukov, Y. D. Chong, C. Martijn de Sterke, "Coherent perfect absorption and reflection in slow-light waveguides," Optics Letters **38(23)**, 4970-4973 (2013).
[20] Wenjie Wan, Y. Chong, Li Ge, Heeso Noh, A. D. Stone, Hui Cao, "Time-Reversed Lasing and Interferometric Control of Absorption" Science **331**, 889-892 (2011).
[21] Shourya Dutta-Gupta, O. J. F. Martin, S. Dutta Gupta, G. S. Agarwal, "Controllable coherent perfect absorption in a composite film," Optics Express **20(2)**, 1330-1336 (2012).
[22] Mingbo Pu, Qin Feng, Min Wang, Chenggang Hu, Cheng Huang, Xiaoliang Ma, Zeyu Zhao, Changtao Wang, Xiangang Luo, " Ultrathin broadband nearly perfect absorber with symmetrical oherent illumination," Optics Express **20(3)**, 2246-2254 (2012).
[23] Jianfa Zhang, Chucai Guo, Ken Liu, Zhihong Zhu, Weimin Ye, Xiaodong Yuan, Shiqiao Qin, "Coherent perfect absorption and transparency in a nanostructured graphene film," Optics Express **22(10)**, 12524-12532 (2014).
[24] Jianfa Zhang, Kevin F. MacDonald and Nikolay I Zheludev, "Controlling light-with-light without nonlinearity," Light: Science & Application **1**, 1-5 (2012).
[25] Nanfang Yu, Federico Capassso, "Flat optics with designer metasurfaces," Nature Materials **13**, (2014).
[26] S. Fan, W. Suh, J. D. Joannopoulos, "Temporal coupled-mode theory for the Fano resonance in optical resonators," J. Opt. Soc. Am. A **20 (3)**, 569-572 (2003).
[27] W. Suh, Z. Wang, S. Fan, "Temporal Coupled-Mode Theory and the Presence of Non-Orthogonal Modes in Lossless Multimode Cavities," IEEE Journal of Quantum Electronics **40(10)**, 1511 -1518 (2004).
[28] M. Kang, Yongnan Li, Hui-Tian Wang, "Fingerprints of topological defects in a metasurface," Optics Letters **39 (16)**, 4879-4882 (2014).
[29] M. Kang, Y. D. Chong, H. T. Wang, W. W. Zhu, M, "Premaratne Critical route for coherent perfect absorption in a Fano resonance plasmonic system," Applied Physics Letters **105**, 131103 (2014).
[30] Sanjay Debnath, Emroz Khan, Evgenii E. Narimanov, "Incoherent perfect absorption in lossy anisotropic materials," Optics Express **27(7)**, 9561- 9569 (2019).
[31] Tae Young Kim, Md. Alamgir Badsha, Junho Yoon, Young Chul Jun, Chang Kwon Hwangbo, "Design of Epsilon-Near-Zero Coherent Perfect Absorption with Indium Tin Oxide Thin Films Using Admittance Matching Method," Conference on Lasers and Electro-Optics Pacific Rim (2015): paper *27P_62*.
[32] Tae Young Kim, Md. Alamgir Badsha, Junho Yoon, Seon Young Lee, Young Chul Jun, Chang Kwon Hwangbo, "General Strategy for Broadband Coherent Perfect Absorption and Multi-wavelength All-optical Switching Based on Epsilon-Near-Zero Multilayer Films," Scientific Reports **6**, 22941 (2016).
[33] Junho Yoon, Md. Alamgir Badsha, Tae Young Kim, Young Chul Jun, Chang Kwon Hwangbo, "Tunable and Broadband Perfect Absorption in Epsilon-Near-Zero Indium Tin Oxide Thin Films at Near Infrared Wavelengths," Conference on Lasers and Electro-Optics Pacific Rim. (Optical Society of America, 2015): paper *26I2_2*.

 © Sociedad Española de Óptica

[34] Junho Yoon, Ming Zhou, Md. Alamgir Badsha, Tae Young Kim, Young Chul Jun, Chang Kwon Hwangbo, "Broadband Epsilon-Near-Zero Perfect Absorption in the Near-Infrared," Scientific Reports **5**, 12788 (2015).
[35] Roman Bruck, Otto L. Muskens, "Plasmonic nanoantennas as integrated coherent perfect absorbers on SOI waveguides for modulators and all-optical switches," Optics Express **21 (23)**, 27662-27671 (2013).
[36] E. Moncada-Villa, Osvaldo N. Oliveira, Jr., and J. R. Mejía-Salazar, "ε-Near-Zero Materials for Highly Miniaturizable Magnetoplasmonic Sensing Devices," J. Phys. Chem. C **123**, 3790−3794 (2019).
[37] J. R. Mejía-Salazar, and Osvaldo N. Oliveira, Jr., "Plasmonic Biosensing Focus Review," DOI: 10.1021/acs.chemrev.8b00359.
[38] J. A. Girón-Sedas, F. Reyes Gómez, Pablo Albella, J. R. Mejía-Salazar, and Osvaldo N. Oliveira Jr., "Giant enhancement of the transverse magneto-optical Kerr effect through the coupling of ε-near-zero and surface plasmon polariton modes," Physical Review B **96**, 075415 (2017).
[39] P. Yeh, *Optical Waves in Layered Media*, Wiley (2005).
[40] H. A. Macleod. *Thin-Film Optical Filters,* 4th edition, London, Taylor & Francis (2010).

1. Introduction

The material which belongs to nearly zero electric permittivity ($\varepsilon \to 0$) at a certain frequency is termed as the epsilon-near-zero (ENZ) material. Unconventionally, lower value of imaginary part $Im(\varepsilon)$ of the ENZ material can produce perfect absorption by trapping infinitely large amount of electric field inside the ENZ thin film [1]. This ENZ absorption property can be extracted in different way of thin film geometry. We analyze here the ENZ CPA in thin film of indium tin oxide (ITO) in asymmetric and symmetric structure as like insulator-metal-insulator (IMI) waveguide.

Transparent coducting oxides (TCOs) are supposed to consider as the alternative of noble plasmonic materials [2]. Usually ENZ properties are to search in periodic 2D and 3D metamatrials (MMs) at the NIR, IR or microwave regimes. It is not rare to extract this property even in visible and infrared region in theoretical and experimental approaches of MMs [3-6]. These nanostructured ENZ MMs are being used in tunneling the electric field and for the transformation of the wavefront with small phase variation [7-14] or in optical cloaking [15]. Beyond the high loss in thicker film, nowadays perfect absorption is to search in the thin ENZ MM [16, 17]. In contrary of enhanced transmission, CPA can be harvested in the ENZ regime [18]. Applying the two inputs propagation system in opposite direction, CPA is analyzed theoretically and demonstrated [19-24] in thin film resonator. Controlling the light in phase and spatial distributions may be the alternative way throughout the CPA even in 2D periodic subwavelength structure like metasurface [25]. In multiport input system, the sharply falling dip of CPA such as the temporal-coupled mode theory (TCMT) [26, 27] can also be comparable with bilayer design of ENZ CPA thin film. Even in critical coupling phenomenon, this CPA mode is also analyzed in the dipole like metasurface and metamaterial of gold [28, 29]. On the other hand, incoherent perfect absorption is found in absorbing anisotropic dielectric slab [30].

Previously CPA is analyzed in ENZ thin film [1, 31]. The tunable and broadband perfect absorptions (BPA) are analyzed also in multilayer of ITO [32, 33]. BPA is demonstrated experimentally in multilayer of ENZ ITO [34]. We employ the absorbing property of ENZ ITO. Regarding this, simply the bilayers of ENZ CPA thin film design are used in near infrared regime, avoiding the complex nanostructured MMs, tunable and multilayer of ENZ ITO. Here a dielectric layer is added with an ENZ ITO layer. The nonabsorbing dielectric layer is used for enhancement of the absorption for obtainment of sharply single dip. The role of incident medium is studied for thinner absorbing film. The analysis is done by admittance matching method and scattering matrix method. The results are also verified by alternative method of CPA conditions. The simulation results show well matching with the developed theories. The right thickness and incident angle are obtained from the admittance matching method for the respective materials in this thin film structure. Controlling the relative phase between the counter incoming beams, this simple geometry has potential applications in optical switch [19] and integrated modulator [35]. It can also be employed in coherent detector [22], sensing device by magnetoplasmonic structure in irfrared to visible spectrum [36, 37] and biosensing device by excitation of SPR [38].

 © Sociedad Española de Óptica

2. CPA Theory in Admittance Matching Method

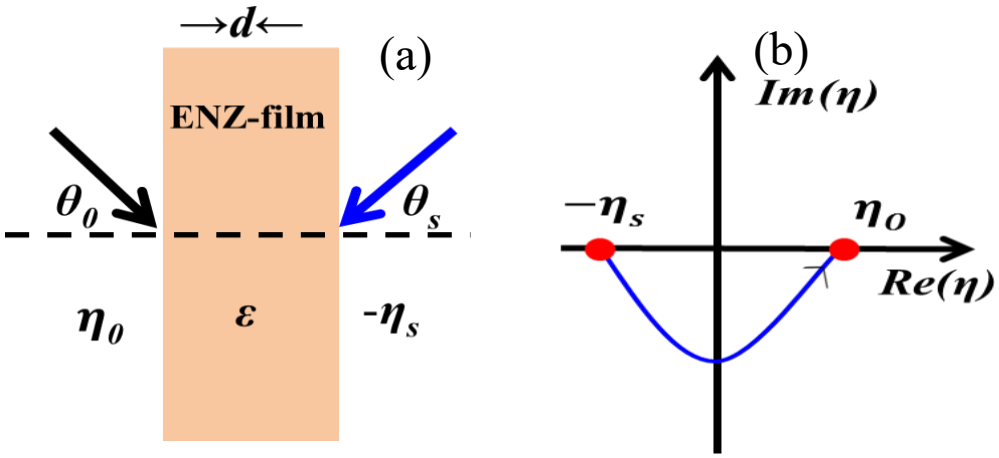

Fig. 1. (a, b) A schematic diagram shows the admittanc matching method for an asymmetric single layer of ENZ CPA.

Admittance matching method is easily applicable to extract an optimum design with the required parameters for a specific optical device than other method. This theory is effective at matching of surface admittance ($Y = \frac{C}{B}$) with the admittance of incident medium (η_0). It causes zero reflectance ($R = 0$) and transmittance is vanished ($T = 0$) at destructive interference at the certain wavelength. It produces the complete effect of absorption. We determine an asymmetric structure by the admittance matching method at p-polarized lihgt using the schematic Fig.1 (a, b). A single absorbing ENZ thin film is shown geometrically in Fig. 1 (a). Obliquely two incoming beams are incident simultaneously from opposite direction of the same film. The forward beam lies in the incident medium at θ_0 degree and the backward beam appears at θ_s degree from the substrate. The forward and backward beams are different in color due to their phase differences which is satisfied the condition of destructive interference in respective medium [23, 32]. The admittance matching diagram is drawn in a complex plane of modified admittance of substrate as shown schematically in Fig.1 (b). The forward locus of admittance starts at real value of coordinates $(-\eta_s, 0)$ and traverses through the complex plane and finally it ends also at the real value of the coordinates $(\eta_0, 0)$. The coordinates of end points of the locus are matched with the real value admittances of substrate $(-\eta_s)$ and incident medium (η_0) respectively. This phenomenon provides the completion of admittance matching design for CPA in a single layer. In this regard, the transfer matrix can be written as:

$$\begin{bmatrix} B \\ C \end{bmatrix} = \begin{bmatrix} \cos\delta & i\frac{\sin\delta}{\eta_f} \\ i\,\eta_f \sin\delta & \cos\delta \end{bmatrix} \begin{bmatrix} 1 \\ -\eta_s \end{bmatrix} \tag{1}$$

where B and C are the normalized electirc field and magnetic field respectively, $\delta = \frac{2\pi d}{\lambda}(n - ik)\cos\theta$ is the optical thickness and $\eta_f = \frac{N_f^2}{N_f cos\theta}$ is the admittance of thin film medium, d is the physical thickness of the thin film, $N_f = n - ik$ is the refractive index of the thin film, n is the real part of refractive index, k is the extinction coefficient, θ is the transmission angle of refracted beam inside the thin film, $\eta_s = \frac{n_s^2}{n_s cos\theta_s}$ admittance of substrate, n_s is the refractive index of substrate, the reversibility of Poynting vector in time-reversal effect is attributable for negative value of substrate admittance $(-\eta_s)$ and $\eta_0 = \frac{n_0^2}{n_0 cos\theta_0}$ admittance of the incident medium, n_0 is the refractive index of incident medium. The tilted admittances of η_f, η_s, η_0 are obtained for p-polarized light.

The Snell's law is defined for multi-layer case as:

$$n_0 \sin\theta_0 = (n - ik)\sin\theta = \cdots \ldots \ldots \ldots = n_s \sin\theta_s \tag{2}$$

 © Sociedad Española de Óptica

Using the eq. (1) the admittance matching satisfies as the surface admittance $\left(such\ as,\ Y = \frac{C}{B} = \eta_0\right)$ and its the simplified expression [32] is derived as:

$$\tan\delta = -i\frac{\eta_f(\eta_0+\eta_s)}{\left(\eta_f^2+\eta_0\eta_s\right)} \tag{3}$$

The eq. (3) is the two counter inputs CPA mode condition at oblique incidence in admittance matching method. The transverse resonance condition of CPA in the absorbing film can be written in the guided mode [39] expression from eq. (3) as-

$$=> 2\delta = 2\tan^{-1}\left(\frac{\eta_f}{i\eta_0}\right) + 2\tan^{-1}\left(\frac{\eta_f}{i\eta_s}\right) + 2m\pi \tag{4}$$

where $\delta = \kappa_f d$ is transverse phase, the inverse of tangents are reflection phases in incident and substrate medium respectively.

The eq. (4) is a single mode resonance and at the thinnest thickness for this mode can be obtained at zero order $m = 0$. Thus admittance matching CPA mode in thin film structure behaves as insulator-metal-insulator (IMI) waveguide and similarly this resonance equation also obtainable for symmetric structure.

Using scattering matrix and admittance matching theory the output amplitudes in incident and substrate medium can be deduced [32] as

$$\begin{bmatrix} O_1 \\ O_2 \end{bmatrix} = \begin{bmatrix} r_1 & \sqrt{\frac{\eta_s}{\eta_0}}\,t_1 \\ \sqrt{\frac{\eta_0}{\eta_s}}\,t_1 & r_2 \end{bmatrix} \begin{bmatrix} 1 \\ \sqrt{\frac{\eta_0}{\eta_s}\,\frac{P_{in2}}{P_{in1}}}\,e^{i\phi_{12}} \end{bmatrix} \tag{5}$$

where r_1, r_2 are reflection coefficients in incident and substrate médium respectively, t_1 is the transmission coefficient, ϕ_{12} is the difference between two counter input beams and $\frac{P_{in2}}{P_{in1}}$ is their irradiance ratio.

The output irradiances in incident and substrate medium can be obtained from eq. (5) as

$$P_{out1} = \frac{1}{2}y_0\eta_0|O_1|^2 = \frac{1}{2}y_0\eta_0\left(R_1 + \frac{P_{in2}}{P_{in1}}\ T_1 + 2\sqrt{\frac{P_{in2}}{P_{in1}}}\sqrt{R_1T_1}\cos\Delta_1\right) \tag{6}$$

where the forward phase relationship can be written as $\Delta_1 = \phi_{r_1} - \phi_{t_1} - \phi_{12}$

Similarly, the interference equation for substrate medium is derived as

$$P_{out2} = \frac{1}{2}y_0\eta_s|O_2|^2 = \frac{1}{2}y_0\eta_0\left[T_1 + \frac{P_{in2}}{P_{in1}}\ R_2 + 2\sqrt{\frac{P_{in2}}{P_{in1}}}\sqrt{R_2T_1}\cos\Delta_2\right] \tag{7}$$

where the backward phase relationship can be written as $\Delta_2 = \phi_{t_1} - \phi_{r_2} - \phi_{12}$

Thus applying these eq. (3, 6, 7), the CPA mode can be obtained in asymmetric and symmetric structures like a guided mode resonance CPA respectively at oblique angle incidence.

3. Simulation Results Analysis of CPA in ENZ Thin Film

3. a. CPA designed by modified admittance in a single layer

This subsection is a test case. The eq. (3) is to apply for CPA study in single layer of ITO thin film at p-polarized light. The symmetric structure is used at unity refractive index ($n_0 = n_s = 1$) for incident and substrate medium. The design is produced at 1369 nm coherent wavelength. The illumination direction is extracted at 70^0 for 118.2 nm thickness. In order to obtain the perfect admittance matching locus in that structure, the coordinates of starting and ending points should be the real value of the substrate admittance as -1 and $+1$ respectively. The locus is little incomplete as it is shown in the Fig. 2 (a). In transfer matrix method (TMM) [40], the coordinate of ending point of modified admittance of substrate is estimated as $0.7487 - i0.4714$. In this state, 97% absorption is achieved as the Fig. 2 (b) is shown. It is obsereved that 3% radiation leakage occurs here. This is a drawback of this design.

 © Sociedad Española de Óptica

By controlling the relative phase, CPA is also investigated as shown in the Fig. 2 (c). If the relative phase is shifted additionally to 90^0 from the irradiance matching condition then absorption reduces. When it is shifted to 180^0 then broadband near infrared input spectrum transparency state is observable in the range of 1200-1500 nm. This is one of the indication as the application of this design as the phase controlled optical switch in near infrared regime.
The relative phase shift is studied in Fig. 2 (d). It is carried out by modulating relative input irradiance ratio (P_{in2}/P_{in1}) of eq. (6, 7). The effect is noticeable in variation of that input ratio at 0.2 and 0.5. The broadband CPA develops perfectly to the longer wavelength of near infrared regimes such as $1420 - 1440\ nm$ and $1400 - 1420\ nm$ wavelength ranges respectively.

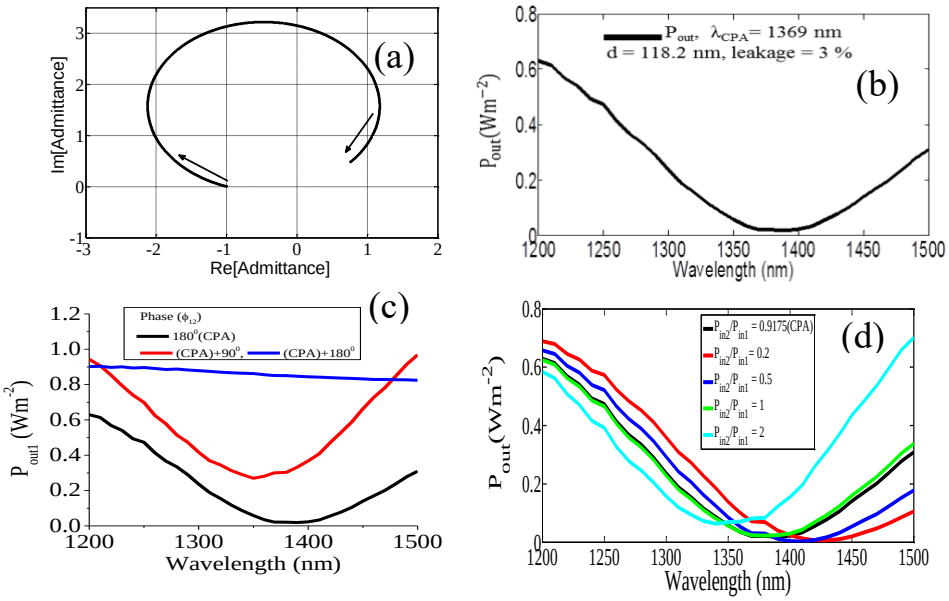

Fig. 2. (a) Admittance matching locus in two inputs CPA design at oblique incidence in a single layer of symmetric structure $(n_0 = n_s)$ such as [Air/ITO/Air] structure, (b) The normalized irradiance spectra in incident medium as P_{out1} is plot theoretically, (c) The normalized frontface irradiance P_{out1} is drawn as function of relative phase shift (φ_{12}) and relative input irradiance ratio of (P_{in2}/P_{in1}).

The CPA is retarded at greater value of relative input ratios (such as for $1, 2$) than the existing CPA value as presented here. Thus in efficient modulation of the relative input ratio at constant phase, CPA is obtainable without radiation leakage in the near infrared regime longer than 1369 nm. This can also be obtained in different way of controlling direction of illumination in different geometries which are being discussed below.

3. b. CPA designed by modified admittance in asymmetric structure

In the previous subsection of (3. a), the symmetric single layer admittance matching design produces almost 97 % absorption. It is achieved perfectly 100 % by addition of a coupling layer in this subsection of (3. b). It appears at longer wavelength than the prior single layer. It shifts to 1435 nm ENZ wavelength of ITO. The additional dielectric layer is convenient to control the phases of incoming two waves from opposite direction and hence the coupling phases of reflection and transmission coefficients are achieved in frontface and backface regions. Thus the structural precision of controlling phase leads to the destructive interference [20] in the incident and substrate medium. The admittance matching design of Ta_2O_5 $(n_1 = 2.1)$ and ENZ ITO $(n_2 = 0.425 - 0.42i)$ is shown in the Fig. 3 (a) at 78.7_0 degree incident angle from air whereas substrate is absorption free BK7 glass $(n_{Sub} = 1.5021)$.
Using this structure, the admittance matching diagram of Fig. 3 (b) is drawn. It is the function of physical thickness and hence the optical phase thickness of the respective thin films in the structure. The coordinates of the starting points of the loci are the real value of modified admittance of substrates for each incoming wave. Similarly, the coordinates of termination points of the loci are the real value of the modified admittance of the incident media from opposite direction. In multilayer, these terminations are taken place by traversing the loci through a common complex coordinate or the coupling coordinate of the complex plane of substrate admittance. The merging of the loci by this coupling produces a single locus as

 © Sociedad Española de Óptica

shown in this diagram. It is the completion of design for obtainment of theoretical CPA mode in a multilayer asymmetric structure.

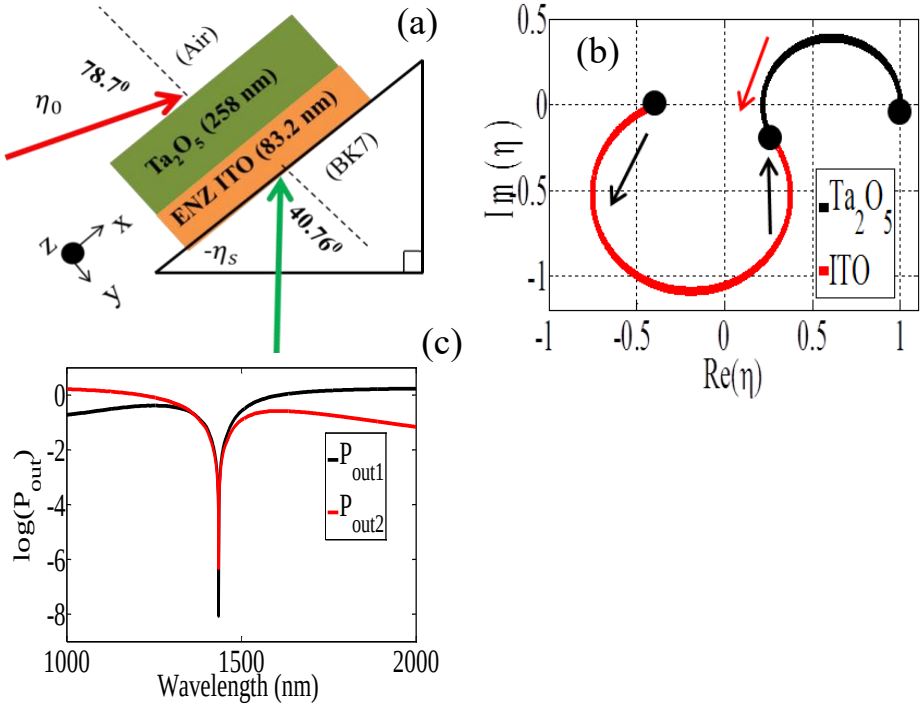

Fig. 3. (a) Schematic of two inputs CPA design in asymmetric structure (b) Admittance matching diagram of structure (a) at 1435 nm ENZ wavelength of ITO and (c) The normalized frontface and backface irradiances are calculated as function of wavelength.

The coordinate of forward locus (red line) launches at the modified admittance of (-0.39184, 0) of real axis of glass substrate. It traverses throughout the absorbing medium of ITO. The coordinate of backward locus (black line) switches at (1, 0) of real axis of air substrate admittance. It passes through the phase controlling dielectric medium of Ta_2O_5. The thin film of dielectric is absorption free as shown in the Fig. 3 (b). Coupling takes place in the interface of ITO-Ta_2O_5. Thickness of the respective thin film and incident angle are obtained from this coupling diagram. These values are shown in Fig. 3(a).

The radius of admittance locus in absorbing thin film depends on thickness [40]. The radius is greater if thickness of absorbing film is lower and vice versa. The second input beam should be inclined at 40.76_0 degree from the substrate medium simultaneously with respect to the first input beam from air as the Snell's law. The CPA design is sensitive to the incoming coherent wavelength, direction of input fluxes and the physical thickness of the thin film.

Using the analytical output irradiance expressions of eq. (6, 7), the normalized outputs are presented in Fig. 3 (c) in logarithmic scale. The normalized irradiances are calculated as the function of wavelength at incident and substrate medium for this structure as the black line and the red line respectively. The output irradiances at CPA wavelength are shown nearly zero. Beyond the phase and irradiance matching, the scattered irradiance enhances and reduces the absorption gradually as incoherent incoming input waves increasing. This occurs as the enhancement of constructive inference. This is the indication of a modulator application of counter-inputs CPA. Irradiance spectra in lower and higher ranges beyond the CPA wavelength are deviated little in forward and backward inputs because of asymmetric structure effect.

We compare the CPA conditions in admittance matching and scattering matrix methods separately. Two alternative methods are applied here to verify the CPA conditions. One is matching relation of reflection and transmission coefficients and another is corresponding phase matching relation. The Fig. 4 (a) represents graphically at variable wavelength, the product of magnitude of reflectance in each medium (black curve) and transmittance (blue curve) $\left(T = \sqrt{R_1 R_2}\right)$. The each of these spectra is distinguishable by means of their characteristics. These spectra show the single intersection coordinate which is corresponding to the CPA wavelength. They carry the same magnitude and hence the coupling condition satisfies at the minimum value of transmittance and the maximum or peak value of reflectance. This resonance coupling produces the destructive interference effect as CPA at coherent wavelength of phase

 © Sociedad Española de Óptica

matching condition. Beyond the resonance wavelength constructive interference enhances as the transmittance spectrum show which is a single dip.

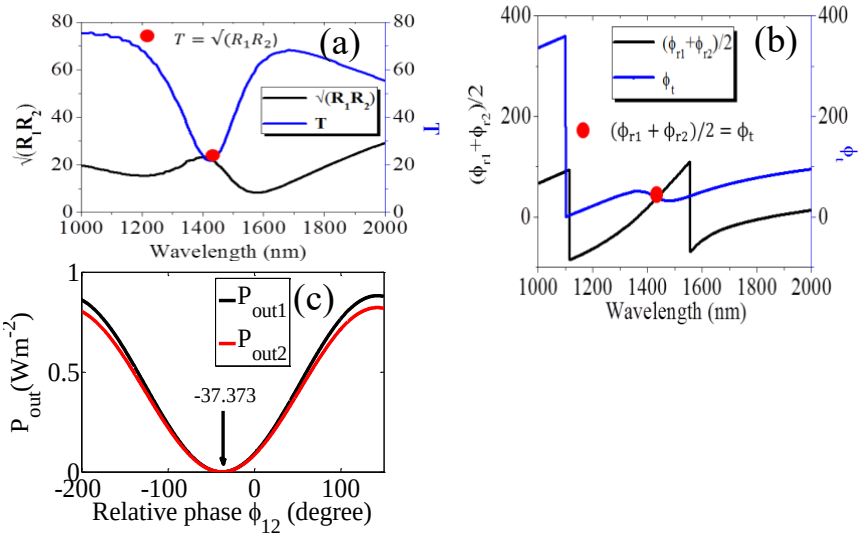

Fig. 4. (a) The two inputs CPA condition is satisfied at magnitude of transmittance and reflectance relationship and (b) Similarly two inputs CPA condition is also satisfied by phase relationship of reflection and transmission coefficients. (c) The normalized frontface and backface irradiances of P_{out1} and P_{out2} are drawn as function of relative phase shift (φ_{12}).

The opposite phenomena occur in case of spectrum of reflectance especially around the resonance wavelength. The Fig. 4 (b) shows the phase relationship of reflection coefficients and transmission coefficient ($\phi_t = (\phi_{r1} + \phi_{r2})/2$). The total reflection phase of incident and substrate medium slightly falls as wavelength increases which is noticeable around the CPA wavelength. Expectedly, at the same spectral position, opposite phenomenon occurs in case of transmission phase. The intersection point of both phases is located in this regime which is also corresponding to the CPA. In these ways the phase matching conditions are satisfied separately.

The output irradiances are also plot in Fig. 4 (c) as function of relative input phase in CPA wavelength. It shows that beyond the relative phase of -37.373$_0$ in degree of CPA mode, the irradiances increase as the effect of constructive interference between scattered amplitudes in each output medium. The sensitivity of relative phase between two inputs is obvious. This property is suitable to optical filter or optical switching applications.

3. c. CPA designed by modified admittance in symmetric structure by BK 7 glass

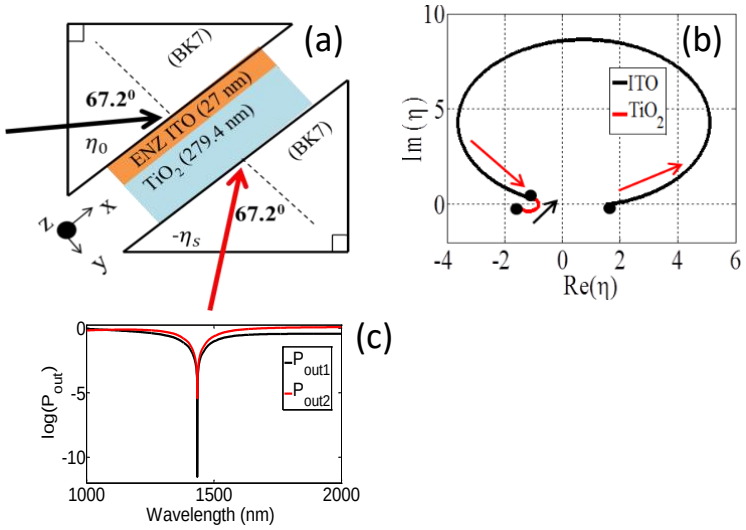

Fig. 5. (a) Schematic of two inputs CPA design in same incident and substrate medium as BK7 glass (b) Admittance matching diagram of structure (a) at 1435 nm ENZ wavelength of ITO and (c) The normalized frontface and backface irradiances are calculated as function of wavelength.

 © Sociedad Española de Óptica

In this subsection of (3. c), we try to extract a suitable angle of the polarizing wave from the incident médium at the ENZ wavelength of ITO. In this consideration BK7 glass ($n_0 = n_{sub} = 1.5021$) is selected as incident and substrate medium for designing another CPA structure as shown in the Fig. 5 (a). A coupling layer of absorption free dielectric material of TiO_2 ($n_1 = 2.25$) is added in this regard. The admittance matching design is achieved at 67.2 degree incident angle in the geometry as shown the Fig. 5 (b). In this structure, the coordinates of forward locus (red line) start at the modified admittance of real axis point (-1.5021, 0) of the substrate. It traverses throughout the phase controlling medium of TiO_2. The coordinates of backward locus (black line) switch at the modified admittance of real axis point (1.5021, 0) of the incident medium of glass. It passes through the absorbing layer of ITO. In this structure obtained thickness of dielectric is 279.4 nm and absorbing layer is 27 nm. Noticeably, denser symmetric incident media and lower illumination angles cause the thinner absorbing layer than previous one. This lower thickness causes higher radius of modified admittance locus throughout this médium as the theory of admittance diagram [40].
Using the same analytical CPA expressions of eq. (6, 7) for this structure the Fig. 5 (c) is plot in logarithmic scale. The normalized irradiances are calculated as function of wavelength at incident and substrate medium for this bilayer layer as the black line and the red line respectively. The irradiances at CPA wavelength are shown nearly zero. Thus the condition of destructive interference is satisfied in forward and backward medium of such symmetric structure at the coherent wavelength.

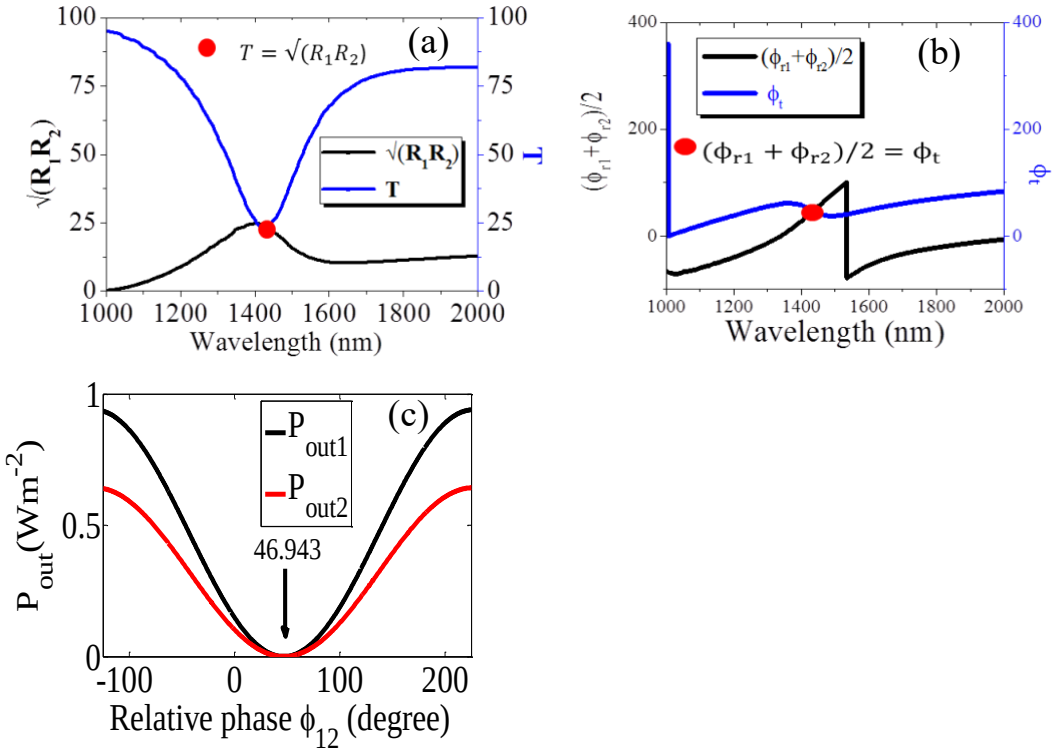

Fig. 6. (a) The two inputs CPA condition is satisfied at magnitude of transmittance and reflectance relationship and (b) Similarly two inputs CPA condition is also satisfied by phase relationship of reflection and transmission coefficients. (c) The normalized frontface and backface irradiances of P_{out1} and P_{out2} are drawn as function of relative phase shift (φ_{12}).

In order to search for the nature of transverse resonance mode, the alternative methods are also applicable to verify the CPA conditions for this structure. The Fig. 6 (a) represents graphically at variable wavelength, the product of magnitude of reflectances in each medium (black curve) and transmittance (blue curve)$\left(T = \sqrt{R_1R_2}\right)$. These spectra show the single intersection coordinate which is corresponding to the CPA wavelength. This is related to resonance effect as satisfaction of the coupling condition.
The Fig. 6 (b) shows the phase relationship of reflection coefficients and transmission coefficient $(\phi_t = (\phi_{r1} + \phi_{r2})/2)$. The intersection point of both phases is located in this regime which is also corresponding to the CPA wavelength as the phase matching condition.
The output irradiances are also plot in Fig. 6 (c) as function of relative input phase in CPA wavelength. It shows that beyond the relative phase of 46.943 in degree of CPA mode, irradiances changes and the sensitivity of relative phase between two inputs is obvious.

 © Sociedad Española de Óptica

3. d. CPA designed by modified admittance in symmetric structure by ZnSe glass

Using the same ENZ wavelength of ITO, we further try to illuminate the polarizing wave searching for the optimum angle from the incident medium. In this consideration, the densest medium of ZnSe ($n_0 = n_{sub} = 2.44903$) is selected to achieve symmetric outputs as the designed Fig. 7 (a). A coupling layer of absorption free dielectric material of SiO_2 ($n_1 = 1.4454$) is added to this ENZ ITO layer. The admittance matching diagram of dielectric and absorbing layer is shown in the Fig. 7 (b) at 45 degree incident angle. As described previously, in this structure the coordinates of forward locus (red line) start at the modified admittance point (-2.44903, 0) of real axis of substrate ZnSe. It traverses throughout the absorption free dielectric medium of SiO_2. The coordinates of the backward locus (black line) switch at the modified admittance another point (2.44903, 0) of real axis of incident medium ZnSe. It passes through the absorbing medium of ITO. In this structure calculated thickness of dielectric is 23.2 nm and that for absorbing layer is 15.62 nm.

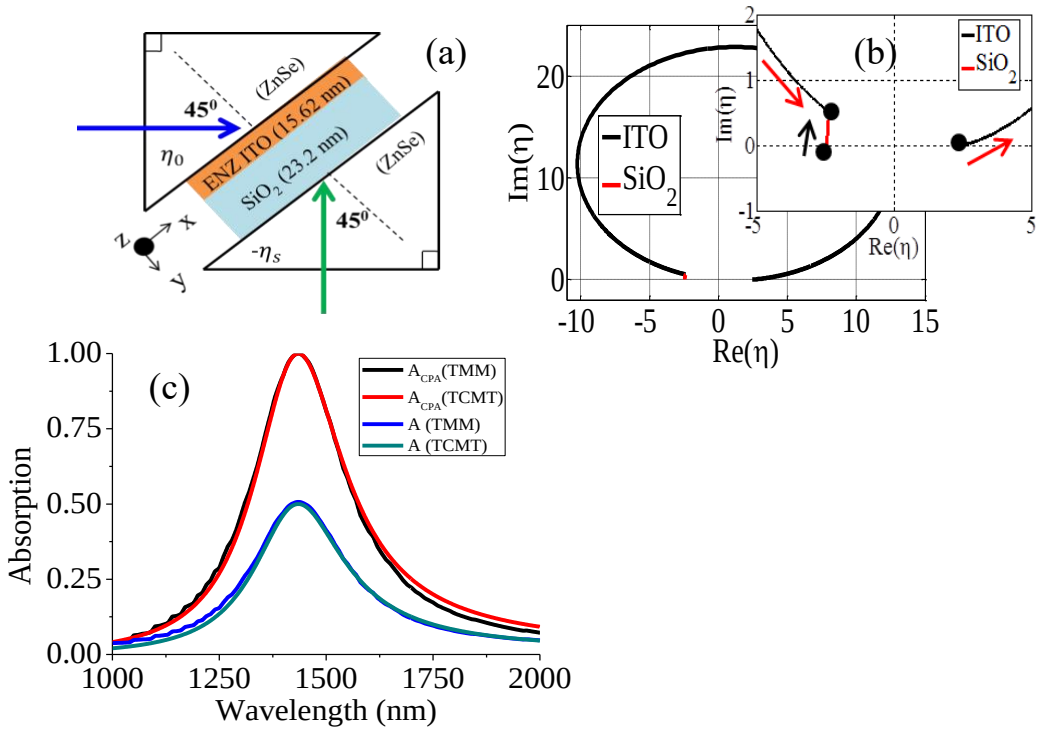

Fig. 7. (a) Schematic of two inputs CPA state in same incident and substrate medium of ZnSe. (b) Admittance matching diagram of structure (a) at 1435 nm ENZ wavelength of ITO. (c) The comparison of two inputs CPA and one input conventional plasma resonance absorption (PRA) between admittance matching method and temporal coupled-mode theory [TCMT] [38, 39].

Remarkably, the densest incident media cause the thinnest absorbing layer than previous subsections of (3. a), (3. b), and (3. c). It indicates the necessity of suitable geometry for ENZ CPA. This Fig. 7 (b) is the extended view of admittance matching diagram. It shows clearly, the interconnectivity between the forward and backward loci as the completeness of admittance matching process. It clarifies the coupling coordinates of the design. Here the design of two counter inputs CPA is confirmed with respect to thickness and incident angle.

The theoretical CPA is compared between TMM (black line) and TCMT (red line) [26, 27] by the Fig. 7 (c). The CPA is greater than 99% at the resonance wavelength in each case. These spectra show well matching. The symmetrical characteristics of the spectra indicate the perfection of denser incident and substrate medium at time-reversal symmetry at near-infrared regime. The Fig. 7(c) also represents these absorption states of one-channel illumination methods. Theoretically it is obtained that for a symmetric structure conventionally 50% absorption occurs due to plasma resonance in absorbing thin film at one way oblique angle input flux. These analytical calculations also match well between the admittance matching method which is calculated by TMM (blue line) and TCMT (olive line) as the conventional absorptions curves. In order to further investigation, previous two alternative methods of phase matching conditions are used to verify the two inputs CPA conditions.

 © Sociedad Española de Óptica

The Fig. 8 (a) represents graphically at variable wavelength, the product of matching coordinates in magnitude of reflectances in each medium (black curve) and transmittance (blue curve). These spectra show the single intersection coordinate which is corresponding to the CPA wavelength 1435 nm. The Fig. 8 (b) shows the phase relationship of reflection coefficients and transmission coefficient. The total reflection phase of incident and substrate medium rapidly falls as wavelength increases which is noticeable around the CPA wavelength at the phase matching condition.

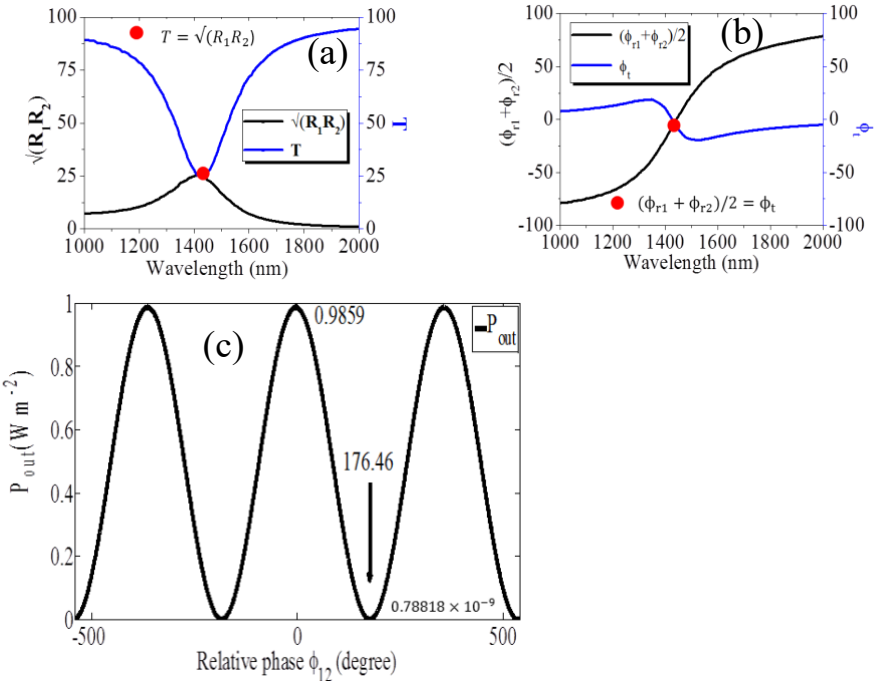

Fig. 8. (a) The two inputs CPA condition is satisfied at magnitude of transmittance and reflectance relationship and (b) Similarly two inputs CPA condition is also satisfied by phase relationship of reflection and transmission coefficients. (c) The normalized máximum and mínimum output irradiances of P_{out} calculated as function of relative phase shift(φ_{12}) of the inputs.

At same absorbing position of wavelength 1435 nm, the completely opposite phenomenon occurs in case of transmission phase throughout the whole range of spectrum. The cross-section point of both phases is located in this regime which is corresponding to the CPA wavelength 1435 nm. In these phase matching methods, the two counter inputs CPA conditions can be satisfied separately.

Table 1: Extraction the feasibility of bilayer admittance matching CPA designs of ENZ ITO.

Input-output medium	Incident angle (degree)	Thickness (nm)		
		ITO	Dielectric materials	
Air-BK7	78.7°	83.2	258	Ta_2O_5
BK7-BK7	67.2°	27	279.4	TiO_2
ZnSe-ZnSe	45°	15.62	23.2	SiO_2

Table 2: Comparison of admittance matching two counter input single and bilayer CPA designs of ENZ ITO.

Optical parameters of ITO	Single layer	Bilayer
CPA rate	97 %	100 %
CPA wavelength	1369 nm	1435 nm
Thickness	118.2 nm	83.2 nm-15.62 nm

The output irradiances are also plot in Fig. 8 (c) as function of relative input phase ϕ_{12} in CPA wavelength. It shows that beyond the relative phase 176.46 in degree of CPA mode, irradiances increase uniformly as the effect of constructive interference between scattered amplitudes in each output medium. The

 © Sociedad Española de Óptica

sensitivity of relative phase between two inputs is obvious. The maximum and minimum output irradiances are calculated 0.9859 and 0.78818×10^{-9} respectively in corresponding peaks and dips as shown in Fig. 8 (c). These are the indications of optical switching and modulation behaviors of this thin film geometry.

The bilayer designs are extracted in Table 1. The effect of incident medium is presented here. It shows the suitability of admittance matching method for CPA thin film design. Considering the polarising direction and thickness, the densest illuminating medium of ZnSe is obtained as optimum for two counter inputs thin film device. Table 2 shows the optical performance of single and bilayer CPA designs. The bilayer designs are mostly feasible for obtainment of desirable optical properties. The fractional values in thicknesses and angles are mentioned just for greater accuracy. The perfect absorption is not hampered without these negligible values.

Thus, using the ENZ CPA property, in integrated optics, chip to chip optical interconnects as modulator can enhance the activities of the future optoelectronics devices (35). In this regard transparent conducting oxide of ENZ ITO may be deserving candidate in telecommunication wavelength in near infrared regime.

4. Conclusion

The absorbing property of ENZ material is employed here to study the CPA. Instead of nanostructured MMs, simply we design bilayers of ENZ CPA thin film in admittance matcing method. A dielectric coupling layer is necessary to deposit on substrate with an ENZ ITO layer in this regard. We analyze these at CPA conditions in admittance matching and scattering matrix methods by amplitudes coefficients and phase matching relationships. For symmetric analysis at optimum polarizing direction of illumination is extracted by subsection 3. d. The agreement was obtained with the admittance matching method and other established method (e.g. TCMT). Controlling the relative phase between the counter input beams, this CPA property of ENZ ITO will be a new way of application in telecommunication regime at asymmetric and symmetric insulator-metal-insulator (IMI) waveguide structures for optical switching and modulation. It can also be employed for infrared sensor.

Acknowledgements

This work is supported by the research project of Jashore University of Science and Technology, Jashore-7408, Bangladesh.

 © Sociedad Española de Óptica